A Unified Fisher's Ratio Learning Method for Spatial Filter Optimization

Xinyang Li, Cuntai Guan, *Senior Member, IEEE,* Kai Keng Ang, *Senior Member, IEEE,* Haihong Zhang, *Member, IEEE*

***Abstract*—To detect the mental task of interest, spatial filtering has been widely used to enhance the spatial resolution of electroencephalography (EEG). However, the effectiveness of spatial filtering is undermined due to the significant non-stationarity of EEG. Based on regularization, most of the conventional stationary spatial filter design methods address the non-stationarity at the cost of the inter-class discrimination. Moreover, spatial filter optimization is inconsistent with feature extraction when EEG covariance matrices could not be jointly diagonalized due to the regularization. In this work, we propose a novel framework for spatial filter design, which is unified with feature extraction as the Fisher's ratio in feature space is directly used as the objective function to optimize the spatial filters. Given its ratio form, the selection of the regularization term could be avoided. We evaluate the proposed method on a binary motor imagery dataset of 16 subjects, who performed the calibration and test sessions on different days. The experimental results show that the proposed method yields improvement in classification performance for both single broad band and filter bank settings compared to conventional non-unified methods. Reduced shifts in test features show more stationary feature distributions obtained by using the proposed method. We also provide a systematic attempt to compare different objective functions in modelling data non-stationarity with simulation studies.**

***Index Terms*—EEG, spatial filtering, BCI, motor imagery, optimization.**

I. Introduction

In discriminative learning of EEG, spatial filtering has been widely applied as preprocessing or feature extraction, especially in EEG-based BCI systems [1], [2]. The function of spatial filtering lies in enhancing the spatial resolution of EEG [3], [4], [5], [6], [7]. Besides, it reduces the number of features as the number of designed spatial filters is usually much less than the number of channels in the scalp space [8]. However, it assumes the stationarity of the spatial distribution of the relevant EEG components over time in spatial filtering. Sensitive to variability in evoked brain responses or human behaviours, EEG recordings usually contain contributions of multiple varying mental processes, only a small portion of which relates to the task of interest. In fact, even resting state brain networks would cause spontaneous fluctuations in the brain signals [9], [10], [3]. The low signal-to-noise ratio and non-stationary nature of EEG significantly undermines the reliability of spatial filtering in enhancing the task-related processes.

The authors are with Institute for Infocomm Research (I2R), Agency for Science, Technology and Research (A*STAR), 1 Fusionopolis Way, 21-01 Connexis (South Tower), Singapore 138632. Email:{lixiy,ctguan,kkang,hhzhang}@i2r.a-star.edu.sg

Many efforts have been made to optimize spatial filter so that it is discriminative while being robust against EEG non-stationarity and artefacts contamination. For instance, common spatial pattern (CSP) analysis is one of the most effective spatial filter design methods for motor imagery discrimination [11], [12]. Given the event-related (de)synchronization (ERD/ERS) in EEG during the imagination of certain movements, CSP extracts the ERD/ERS effects by maximizing the power of the spatially filtered signals for one class while minimizing it for the other class [13], [14]. As the EEG data is in the form of multi-channel time series, the covariance matrix of EEG consists of covariances between EEG signals from pairs of channels. With the class-wise average of the covariance matrices, the objective function of CSP is casted in relation to Rayleigh quotient between the average covariance matrices, which is equivalent to the ratio of powers of the EEG signals from the two classes. The objective function has been used for joint temporal-spatial analysis as an improvement of CSP [8]. In [15], the authors propose discriminative filter bank CSP (DFBCSP), where the finite impulse response (FIR) filters and the associated spatial weights are obtained in a sequential manner by optimizing Rayleigh quotient. In iterative spatio-spectral patterns learning (ISSPL), Rayleigh quotient is combined with the objective function of support vector machine (SVM) to optimize spatio-spectral filters and the classifier in a sequential manner [16]. Similarly, in [17], spatial filters and time-lagged coefficient matrices in a convolutive model are jointly optimized using Rayleigh quotient to address the propagation effects in motor imagery EEG.

The Rayleigh quotient objective function is effective in terms of discrimination, while it is prone to nonstationairty. Thus, a number of regularization methods have been proposed to improve its robustness against the data non-stationarity [18]. The regularization method refers to adding a regularization term to the denominator of the Rayleigh quotient so that this term can be penalized in the objective function [19]. To achieve the invariant property of the spatial filters, stationary CSP is proposed to address nonstationary noise in a more general case without using additional recordings to estimate the nonstationary artefacts [20]. In particular, non-stationarity is estimated as the sum of absolute differences between the mean variance and variance of a certain trial in the projected space. In [21], the nonstationary projection directions are estimated based on the principal component analysis (PCA) using cross-subject data, and then penalized in the objective

function to build subject-specific spatial filters.

In [22], the authors introduce a different penalizing term that measures the Kullback-Leibler divergence (KL-divergence) of the EEG distributions across trials, and subsequently, the objective function can minimize within-class dissimilarities. In [23], different divergence measurements are used as non-stationarity regularization, and it is proved that spatial filters in CSP project the EEG data into subspaces where the KL-divergence between the data distributions from two classes is maximized. Therefore, the objective function of CSP can also be formed in a divergence-based framework. The significance of this work lies in the fact that it is a unified framework for CSP with different kinds of regularization.

Besides Rayleigh quotient and KL-divergence, the mutual information has also been used for spatial filter optimization. In [24], [25], multiple bandpass filters denoted as a filter bank are applied for raw EEG data, and the CSP spatial filters are calculated for each filter band. Thus, each pair of bandpass and spatial filter yields CSP features that are specific to the frequency range of the bandpass filter. Then, both spatial and temporal filters are optimized by selecting those features with higher mutual information with the class labels. Similarly, in the optimum spatio-spectral filtering network (OSSFN), the bandpass filters and spatial filters are jointly optimized to maximize the mutual information between feature vector variables and the class label via gradient searching [26].

Generally, Rayleigh quotient, KL-divergence and mutual information are conventional objective functions for spatial filter optimization, and they are often combined in different ways. As aforementioned, KL-divergence based loss function can be used as a regularization term in the Rayleigh quotient objective function to penalize the within-class dissimilarity, while mutual information is used to select filter bands as a way of temporal filter optimization. However, their relationships with classification in the feature space have not been investigated sufficiently, especially when non-stationarity needs to be taken into consideration. In [27], the authors establish the theory linking Rayleigh quotient with Bayes classification error in the CSP feature space. In that work, the feature non-stationarity is simplified by assuming that the shape parameter of the feature distribution is independent of the spatial filters. As most of the stationary spatial filter design methods are based on regularization, the inter-trial non-stationarity or the within-class dissimilarity is minimized at the cost of inter-class dissimilarity, which can be regarded as one of the limitations of the regularization methods. Moreover, divergence measurements are usually applied in the covariance matrix space rather than in the feature space. The problem lies in the fact that the spatial filters with regularization usually fail to jointly diagonalize the covariance matrices while only the diagonal elements are used as features. In other words, the feature used for classification is not consistent with the optimization objective function in the spatial filter design based on the covariance matrix. Due to the inconsistency, stationarity or discrimination for the covariance matrix cannot be fully transferred into that for the features.

To address the issue, we propose to optimize spatial filers using the Fisher's ratio in the feature space. This is a unified framework for spatial filter design, as it directly addresses discrimination and stationarity in the feature space, compared to objective functions in the conventional spatial filter optimization. Given its ratio form, within-class feature dissimilarity could be minimized without sacrificing inter-class discrimination, and regularization parameter selection could be avoided. Moreover, we provide a systematic attempt to compare the effectiveness of different objective functions by applying them to both feature extraction and selection with single broad band or filter bank as preprocessing. In particular, the roles that different objective functions play in non-stationarity measurement have been investigated and discussed. Based on the above discussion, we highlight the contributions of this paper as follows:

(i) a Fisher's ratio based spatial filter design method is proposed;
(ii) relationships between different objective functions: Rayleigh quotient, KL-divergence and mutual information, are discussed; and
(iii) efficiency of different objective functions in the non-stationarity modelling is investigated.

II. Preliminaries of Spatial Filter Design

TABLE I
NOMENCLATURE

X	band-passed EEG data;
n_c	number of electrodes or channels;
n_t	number of time points;
j	trial index;
i	feature dimension index;
$c \in +, -$	class index;
$\mathcal{Q}^c$	a set containing indexes of trials that belong to class c;
R	covariance matrix of EEG data;
$\bar{R}^c$	average covariance matrix of class c;
W	projection matrix for feature extraction;
$\mathbf{w}$	spatial filter, one row in W;
P	whitening matrix;
U	rotation matrix;
U_m	discriminative subspace;
m	dimension of the discriminative subspace;
J	objective function;
Λ	covariance matrix after projection;
$\mathbf{f}$	variance feature of the EEG signal after projection;
$\mathbf{d}$	feature distance;
λ	regularization parameter;
Δ_s	stationary regularization term;
k	iteration index.

A. Common Spatial Pattern Analysis

Let $X_j \in \mathbb{R}^{n_c \times n_t}$ be the the bandpass filtered EEG data of trial j, where n_c and n_t are the numbers of channels and time points, respectively. As the mean of X_j is zero after the preprocessing, the covariance matrix R_j could be obtained as

$$R_j = \frac{X_j (X_j)^T}{\mathrm{tr}[X_j (X_j)^T]} \tag{1}$$

The CSP spatial filter $\mathbf{w}$ is designed to maximize the variance of the spatially filtered signal under one condition, and given the constraint that the sum of the variances under

two conditions is one, the variance under the other condition could be minimized subsequently. The objective function of CSP can be expressed in the following optimization problem:

$$\max_{\mathbf{w}} \mathbf{w}^T \bar{R}^c \mathbf{w} \quad s.t. \quad \mathbf{w}^T(\bar{R}^+ + \bar{R}^-)\mathbf{w} = 1 \tag{2}$$

$\bar{R}^c$ is the average covariance matrix for class c, i.e.,

$$\bar{R}^c = \frac{1}{|\mathcal{Q}^c|} \sum_{j \in \mathcal{Q}^c} R_j, \ c \in \{+, -\}, \tag{3}$$

where $\mathcal{Q}^c$ is the set containing indexes of trials that belong to class c.

B. Common Spatial Pattern Analysis in KL-divergence Form

Given that EEG data is usually processed to be centered, the KL-divergence between two EEG datasets, i_1 and i_2, is

$$\begin{aligned} & D_{kl}(R^{i_1}||R^{i_2}) \\ = & \frac{1}{2}\left(\mathrm{tr}\left(\left(R^{i_2}\right)^{-1} R^{i_1}\right) - \ln\left(\frac{\det R^{i_1}}{\det R^{i_2}}\right) - n_c\right) \end{aligned} \tag{4}$$

and the symmetric KL-divergence is defined as

$$\tilde{D}_{kl}(R^{i_1}||R^{i_2}) = D_{kl}(R^{i_1}||R^{i_2}) + D_{kl}(R^{i_2}||R^{i_1}) \tag{5}$$

In [23], it is proved the solution of Eq.(2) is equal to that of the following optimization problem, i.e., the spatial filters maximizing the symmetric KL-divergence between the two classes:

$$W = \arg\max_{W} \ \tilde{D}_{kl}(WR^+W||WR^-W^T) \tag{6}$$

The objective function with stationary regularization term, Δ_s, can be formulated as

$$J_{kl} = (1-\lambda)\tilde{D}_{kl}(WR^+W^T||WR^-W^T) - \lambda\Delta_s \tag{7}$$

Δ_s may vary according to the type of non-stationarity to be minimized. Typically, it is the class-wise inter-trial non-stationarity, measured as the class-wise average divergence between the trials and mean data distributions as below

$$\Delta_s = \sum_{c=\{+,-\}} \frac{1}{|\mathcal{Q}^c|} \sum_{j \in \mathcal{Q}^c} D_{kl}(WR_jW^T||WR^cW^T) \tag{8}$$

III. Spatial Filter Optimization Based on Fisher's Ratio

Most of the existing stationary approaches have a similar form as Eq.(7), where different regularization terms are used to penalize the data non-stationarity [20], [22], [21]. One of the limitations of such a formulation is that the data non-stationarity is minimized at the cost of the inter-class dissimilarity. It usually takes cross-validation to find the regularization term λ. To address both the inter-trial non-stationarity and class discrimination in the spatial filter design, in this section, we will introduce the objective functions based on Fisher's ratio.

A. Objective Function based on Fisher's Ratio

The projection matrix W in CSP can also be represented as

$$W = P^T U \tag{9}$$

where each row of W is one solution of Eq.(3), and P is the whitening matrix such that

$$P(\bar{R}^+ + \bar{R}^-)P^T = I \tag{10}$$

Define the covariance matrix after whitening:

$$\bar{\Sigma}^c = P\bar{R}^cP^T \tag{11}$$

Each column of U in Eq.(9), $\mathbf{u}_i, i = 1, ..., n_c$, is an eigenvector of $\bar{\Sigma}^c$. Usually, only those eigenvectors $\mathbf{u}_i$ corresponding to the largest and smallest eigenvalues of $\bar{\Sigma}^c$ are used for feature extraction as the following

$$W = P^T U_m \tag{12}$$

$$U_m = I_m U \tag{13}$$

where U_m can be regarded as the discriminative subspace, m is the dimension of feature and I_m is a m-by-n_c identity matrix. The covariance matrix after projection can be written as

$$\Lambda_j = U_m^T \Sigma_j U_m \tag{14}$$

where

$$\Sigma_j = PR_jP^T \tag{15}$$

Remark 1: As CSP maximizes the power of one class and minimizes it for the other class, the whitening in Eq.(10) is a necessary constraint. Since the proposed optimization framework adopts the Fisher's ratio in the feature space as objective function, the whitening is no longer necessary. However, with the whitening matrix P, features could be normalized to the range around $[0, 1]$, which is beneficial for the classification. Thus, the proposed spatial filter optimization is based on the covariance matrix after the whitening, i.e., Σ.

Then, the feature vector $\mathbf{f}_j \in \mathbb{R}^m$ for trial j extracted by the projection matrix W is

$$\mathbf{f}_j = \mathrm{diag}(\Lambda_j), j = 1, ..., m \tag{16}$$

which contains the variances of the EEG signals after projection. Let the i-th element of $\mathbf{f}_j$ be $\mathbf{f}_{j,i}$. Suppose trial i belongs to class c, and let $\bar{\mathbf{f}}_i^c$ be the mean of the i-th feature of class c. Then, the distance between $\mathbf{f}_{j,i}$ and $\bar{\mathbf{f}}_i^c$ is

$$\mathbf{d}_{j,i} = \mathbf{f}_{j,i} - \bar{\mathbf{f}}_i^c \tag{17}$$

Furthermore, the within-class distance S_w is

$$S_w = \frac{1}{2}\sum_{c \in \mathcal{C}} \frac{1}{|\mathcal{Q}^c|} \sum_{j \in \mathcal{Q}^c} \frac{1}{m} \sum_{i=1}^{m} (\mathbf{d}_{j,i})^2 \tag{18}$$

Similarly, the inter-class distance between the mean features of the two classes is

$$S_b = \frac{1}{m} \sum_{i=1}^{m} (\bar{\mathbf{d}}_i)^2 \tag{19}$$

where

$$\bar{\mathbf{d}} = \bar{\mathbf{f}}^{+} - \bar{\mathbf{f}}^{-} \tag{20}$$

With Eq.(18) and Eq.(19), the Fisher's ratio objective function can be obtained as

$$J_{fs} = \frac{S_w}{S_b} \tag{21}$$

Let $\mathbf{1}_n^i \in \mathbb{R}^n$ be a n-dimenstion vector with the i-th element as 1 and other elements as 0, i.e.,

$$\mathbf{1}_n^i = [0, 0, ..., 1, ..., 0]^T \tag{22}$$

Then, the features can be rewritten as

$$\begin{aligned} \mathbf{f}_{j,i} &= (\mathbf{1}_{n_c}^i)^T \Lambda_j \mathbf{1}_{n_c}^i & (23)\\ \bar{\mathbf{f}}_i^c &= (\mathbf{1}_{n_c}^i)^T \bar{\Lambda}^c \mathbf{1}_{n_c}^i & (24) \end{aligned}$$

Substituting Eq.(14), Eq.(23) and Eq.(24) into Eq.(17), the distance between $\mathbf{f}_{j,i}$ and the mean of features from the same class $\bar{\mathbf{f}}^c(i)$ is

$$\begin{aligned} \mathbf{d}_{j,i} &= (\mathbf{1}_{n_c}^i)^T (\Lambda_j - \bar{\Lambda}^c) \mathbf{1}_{n_c}^i \\ &= (\mathbf{1}_m^i)^T U_m^T \Delta\Sigma_j U_m \mathbf{1}_m^i \end{aligned} \tag{25}$$

where

$$\Delta\Sigma_j = \Sigma_j - \bar{\Sigma}^c, \quad j \in \mathcal{Q}^c \tag{26}$$

Let $\mathbf{1}_n^{ii} \in \mathbb{R}^{n \times n}$ be a n-by-n matrix with the element of the i-th column and i-th row as 1 and other elements as 0, i.e.,

$$\begin{aligned} \mathbf{1}_n^{ii} &= \mathbf{1}_n^i (\mathbf{1}_n^i)^T \\ &= \begin{pmatrix} 0 & 0 & \dots & 0 \\ 0 & \ddots & \dots & 0 \\ \vdots & \vdots & 1 & \vdots \\ 0 & 0 & \dots & 0 \end{pmatrix} \end{aligned} \tag{27}$$

Then, the squared distance is

$$\mathbf{d}_{j,i}^2 = (\mathbf{1}_m^i)^T \left(U_m^T \Delta\Sigma_j U_m \mathbf{1}_m^{ii} U_m^T \Delta\Sigma_j U_m \right) \mathbf{1}_m^i \tag{28}$$

Substituting Eq.(28) into Eq.(18), we have

$$\begin{aligned} S_w &= \frac{1}{2} \sum_{c \in \mathcal{C}} \frac{1}{|\mathcal{Q}^c|} \sum_{j \in \mathcal{Q}^c} \frac{1}{m} \sum_{i=1}^{m} \\ &\quad (\mathbf{1}_m^i)^T \left(U_m^T \Delta\Sigma_j U_m \mathbf{1}_m^{ii} U_m^T \Delta\Sigma_j U_m \right) \mathbf{1}_m^i \end{aligned} \tag{29}$$

Similarly, the inter-class distance between the mean features of the two classes can be obtained as

$$\begin{aligned} S_b &= \frac{1}{m} \sum_{i=1}^{m} (\bar{\mathbf{d}}_i)^2 & (30)\\ &= \frac{1}{m} \sum_{i=1}^{m} (\mathbf{1}_m^i)^T \left(U_m^T \Delta\Sigma U_m \mathbf{1}_m^{ii} U_m^T \Delta\Sigma U_m \right) \mathbf{1}_m^i & (31) \end{aligned}$$

where $\bar{\mathbf{d}}_i$ is the i-th element of $\bar{\mathbf{d}}$, and

$$\Delta\Sigma = \bar{\Sigma}^{+} - \bar{\Sigma}^{-} \tag{32}$$

Substituting Eq.(29) and Eq.(30) into Eq.(21), we can obtain the Fisher's ratio objective function of U_m as

$$\hat{U}_m = \arg\min_{U_m} J_{fs}(U_m) \ s.t. \ U_m^T U_m = I \tag{33}$$

Remark 2: Although Fisher's ratio in Eq.(21) in linear discriminative analysis could be regarded as a kind of Rayleigh quotient, the subspace optimization in Eq.(33) is actually not in Rayleigh quotient form when Eq.(29) and Eq.(30) are substituted into Eq.(21). In this work, Rayleigh quotient objective function refers to the Rayleigh quotient used in CSP, which is equivalent to the ratio between the means of the two classes in the feature space. The difference between Eq.(21) and CSP lies in that CSP only considers the inter-class distance and the Fisher's ratio in Eq.(21) maximizes inter-class distance while minimizing within-class distances.

After optimizing U_m using Eq.(33), the projection matrix can be obtained by substituting $\hat{U}_m$ into Eq.(9). The optimization of the discriminative subspace is accomplished by using gradient descent on the manifold of orthogonal matrices, which is shown in Algorithm 1. Details of the subspace optimization approach can be found in [23], [28].

Algorithm 1: Subspace optimization through gradient searching.

Input: training data with labels;
Output: $\hat{U}_m$.
begin
Compute whitening matrix P;
Compute whitened covariance matrices Σ_j and $\bar{\Sigma}^c$;
Initialize U_m^k as the discriminative subspace in the CSP solution in Eq.(9) to Eq.(12) with $k = 0$.
repeat:
Compute the covariance matrices after rotation Λ^k or features $\mathbf{f}^k$;
With Λ^k or $\mathbf{f}^k$, compute the gradient matrix ∇_{U_m} with respect to $J(U_m)$ and obtain H as:

$$H = \begin{pmatrix} 0 & \nabla_{U_m} \\ -\nabla_{U_m}^T & 0 \end{pmatrix};$$

Given $t_u = [0.9^5, 0.9^6, ..., 0.9^{10}]$, estimate the optimal step size by line search such that

$$\hat{t}_u = \arg\min_{t_u} J_{fs}(U_m^k \exp(t_u H))$$

Update the rotation matrix and the covariance matrix as below

$$U_m^{k+1} = (U_m^k) \exp(\hat{t}_u H)$$

Increase the iteration index as $k \to k + 1$.
until convergence.
end

B. Filter Bank Fisher's ratio Spatial Filtering

In this work, we evaluate the proposed spatial filter optimization method by applying it to EEG signals band-passed by single broad band filter, and a filter bank that consists of multiple filters [24], [25]. Moreover, given the spatial filter optimization based on Fisher's ratio, we propose to conduct

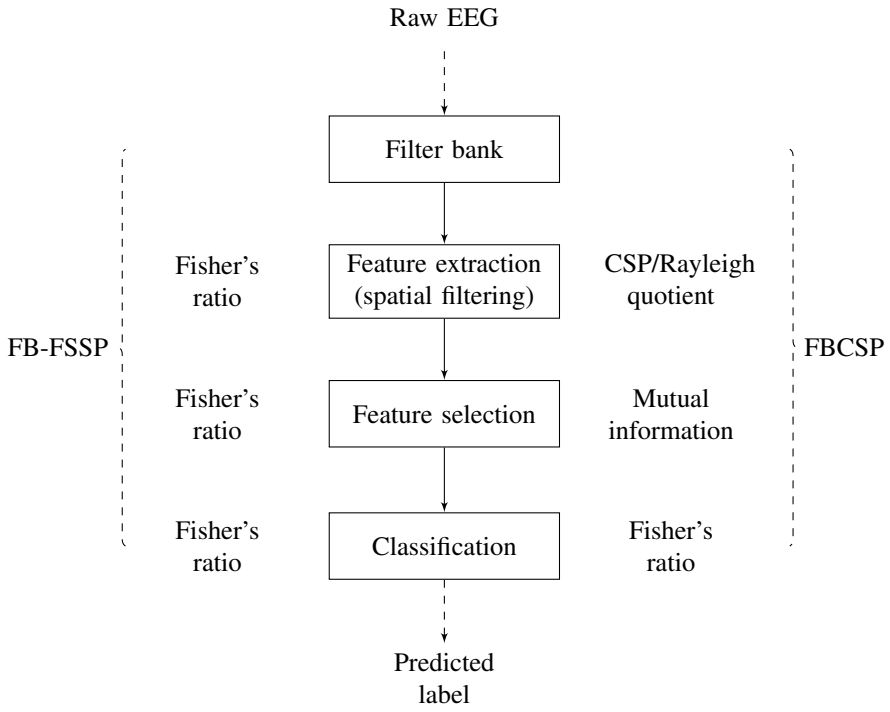

Fig. 1. The flow chart of the EEG signal processing procedures in FB-FSSP and FBCSP.

feature selection also using Fisher's ratio. In the rest parts of the paper, FB-FSSP is used as a shorthand notation for the method combining filter bank and Fisher's ratio spatial filter optimization. The flowchart of the EEG signal processing procedures is shown in Figure 1, where the objective functions used in FBCSP and FB-FSSP for spatial filtering, feature selection and classification steps are annotated for comparison. With Fisher's ratio Eq.(21) as the objective function, the proposed spatial optimization is consistent with the features in Eq.(16) used for feature selection and classification. Compared to FBCSP, the proposed FB-FSSP is a more unified framework also in the sense that Fisher's ratio objective function is used in all the three steps in EEG processing.

IV. Experimental Study

A. Experimental Setup and Data Processing

EEGs from the full 27 channels were obtained using Nuamps EEG acquisition hardware with unipolar Ag/AgCl electrodes channels. The sampling rate was 250 Hz with a resolution of 22 bits for the voltage range of $\pm$ 130 mV. A bandpass filter of 0.05 to 40 Hz was set in the acquisition hardware.

The dataset contains 16 subjects who attended two parts of the experiment on separate days. In the first part, there were one motor imagery session and one passive movement session, each of which contained 2 runs. During the motor imagery session, the data were recorded from subjects performing kinaesthetic motor imagery of the chosen hand or background idle condition. During the passive movement session, EEG data were collected from the subjects with passive movement of the chosen hand performed by a haptic knob robot or performing similar background idle condition. Each run lasted for approximately 16 minutes and comprised 40 trials of motor imagery or passive movement, and 40 trials of idle state. In the second part, there was one motor imagery session consisting of 2-3 runs. During the EEG recording process, the subjects were asked to avoid physical movement and eye blinking. Thus, there are 80 trials per class in the training session and 80-120 trials per class in the test session, yielding totally 160 training trials and 160-240 test trials for each subject. Details of the experimental setup can be found in [29].

With 27 channels of EEG, $n_c = 27$. For each trial, the EEG from the time segment of 0.5s to 2.5s after the cue is extracted, resulting in $n_t = 500$. Single or multiple band-pass filters are applied to the time segment. In particular, for single band setting, the EEG segment is band-passed by a broad band-pass filter of $4-40$Hz, and then spatial filtering as feature extraction is applied with 2 pairs of the spatial filters used. For multiple band setting, we construct 9 temporal band-pass filters, $4-8, 8-12, ..., 36-40$Hz, which have been proved to cover the frequency range with the most distinctive ERD/ERS effects [24], [25]. Similarly, spatial filtering with 2 pairs of the spatial filters is used for each of the 9 frequency bands, yielding totally 36 features. For feature selection, 8 features are selected based on mutual information, Fisher's ratio, or KL-divergence. Finally, feature vectors are classified using a linear discriminant analysis (LDA) classifier.

B. Comparing Different Objective Functions in Feature Selection

In this section, we compare the different objective functions in feature selection. To avoid the regularization coefficient λ in

Eq.(7), we construct a loss function as the ratio of inter-class KL-divergence and the within-class KL-divergence, i.e.,

$$\tilde{J}_{kl} = \frac{\sum_{c=\{0,1\}} \frac{1}{|\mathcal{Q}^c|} \sum_{j \in \mathcal{Q}^c} D_{kl}(WR_jW^T || WR^cW^T)}{\tilde{D}_{kl}(WR_1W^T || WR_0W^T)} \quad (34)$$

The classification results of features selected by different methods are summarised in Table II, where "MI_0" indicates that mutual information based on Parzen window is used for feature selection, "FS" indicates that Eq.(21) is used, and "KL" indicates that Eq.(34) is used. As shown in Table II, "FS" yields better results than that of "MI_0", which is regarded as the baseline method. Note that the results in Table II are based on training and testing the model both by motor imagery EEG.

TABLE II
CLASSIFICATION RESULTS OF USING DIFFERENT FEATURE SELECTION METHODS (%)

	Training Acc.			Test Acc.		
Subject	MI_0	KL	FS	MI_0	KL	FS
1	80.63	88.13	85.63	50.42	52.08	57.08
2	89.17	87.50	95.00	60.42	56.67	51.25
3	84.17	90.83	91.67	52.92	61.67	68.33
4	94.17	95.00	94.17	71.25	57.50	71.25
5	95.00	95.00	90.83	58.75	59.17	60.83
6	97.50	97.50	96.67	83.33	76.67	85.00
7	97.50	91.67	97.50	78.75	58.33	72.92
8	98.33	99.17	98.33	96.25	95.83	96.25
9	94.38	93.13	94.38	69.17	69.58	69.58
10	85.00	86.67	90.83	65.00	60.00	60.42
11	69.17	95.83	92.50	51.25	50.00	51.67
12	92.50	91.67	92.50	79.58	75.83	79.58
13	73.13	83.13	72.50	75.63	49.58	50.00
14	90.63	93.75	94.38	94.38	75.00	74.58
15	91.88	93.75	89.38	91.88	62.92	67.50
16	90.63	92.50	92.50	90.63	71.67	79.58
mean	88.98	92.20	92.03	67.27	64.09	68.49
median	91.25	92.81	92.50	67.08	60.83	68.96

Figure 2 shows the Fisher's ratio and the KL-divergence ratio Eq.(34) of different bands, averaged across all subjects. In Figure 2, the x-axis represents the starting frequency of each band-pass filter, and the blue and red lines represent the Fisher's ratio and the KL-divergence ratio, respectively. Despite the fluctuation in the Fisher's ratio, both the Fisher's ratio and the KL-divergence ratio are lower in the frequency range 8-20Hz, which is known to be the frequency range with stronger ERD/ERS effects. The results of feature selection show the effectiveness of the Fisher's ratio and it is feasible to optimize the spatial filter using it as the objective function.

C. Spatial Filter Optimization

In this section, we evaluate the performance of the spatial filter optimization method proposed in Section III. For a more comprehensive comparison, we also implement the subspace optimization using mutual information as the objective function. To reduce the computational complexity, the mutual information is calculated using single Gaussian function in the optimization process instead of the Parzen window used in FBCSP, and details of the spatial filter optimization can be found in Appendix A. To differentiate the mutual information

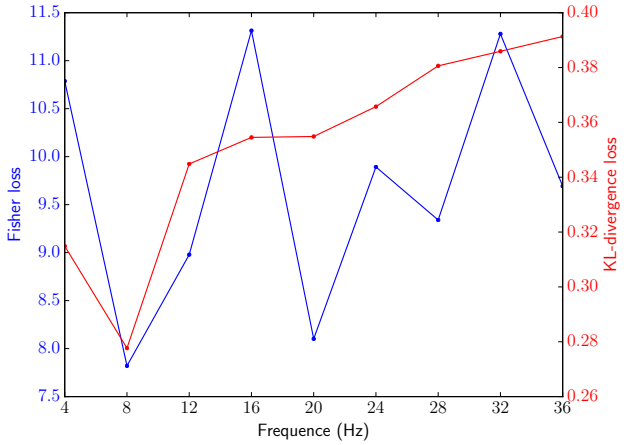

Fig. 2. Comparison between the Fisher's ratio and the KL-divergence ratio.

calculation methods, we use MI_s as the notation of the simplified mutual information objective function. During the subspace optimization procedure described in Algorithm 1, the subspace dimension m is set as half of the number of channels, i.e., $m = 0.5n_c$. Upon the completion of the optimization, 2 pairs of spatial filters are selected via sorting them according to the Fisher's ratio of each feature dimension.

Table III shows the classification results of applying different spatial filter optimization methods proposed to EEG filtered by a single broad band. Note that the results in Table III are based on training and testing the model both by motor imagery EEG. It is found that both spatial filter optimization methods outperform single band CSP, and FS yields the best average classification accuracy.

TABLE III
CLASSIFICATION RESULTS USING SINGLE BROAD BAND (%)

	Training Acc.			Test Acc.		
Subject	CSP	MI_s	FS	CSP	MI_s	FS
1	84.38	88.75	88.75	57.08	66.67	66.67
2	70.83	81.67	81.67	51.25	57.92	55.00
3	67.50	90.83	94.17	57.50	55.83	58.75
4	87.50	94.17	94.17	52.50	51.67	51.67
5	90.00	93.33	93.33	50.83	51.25	51.25
6	90.83	94.17	96.67	65.00	67.92	81.67
7	78.33	86.67	86.67	70.00	72.08	72.08
8	99.17	98.33	98.33	95.00	96.67	96.67
9	88.75	90.00	90.00	72.50	70.00	70.00
10	70.00	78.33	81.67	61.67	59.58	58.33
11	60.83	74.17	76.67	47.50	48.75	52.50
12	90.83	93.33	93.33	81.25	78.33	78.33
13	66.88	67.50	68.13	50.83	50.42	50.00
14	90.00	91.88	91.88	72.50	77.08	77.08
15	85.00	85.00	85.63	64.58	65.42	64.58
16	85.00	90.00	90.00	70.00	70.83	70.83
mean	81.61	87.38	88.19	63.75	65.03	65.96
median	85.00	90.00	90.00	63.13	66.04	65.63

Table IV shows the classification results of applying different optimization methods to EEG filtered by filter bank with different feature selection methods. For mutual information based spatial filer optimization, MI_0 is used for feature selection. Moreover, FB-FSSP is implemented in two manners,

which are denoted as FB-FSSP1 and FB-FSSP2 in Table IV. In FB-FSSP1, Fisher's ratio spatial filter optimization is applied to EEG signals band-passed by filter bank of all 9 frequency bands at the training stage, followed by feature extraction and feature selection. In FB-FSSP2, FBCSP is applied at the first place, and Fisher's ratio spatial filter optimization is only applied to the selected bands for feature extraction. Thus, compared to FB-FSSP1, the computational complexity of FB-FSSP2 is lower. Moreover, 'M" is used to denote using motor imagery data as the training data, and "P" to denote using the passive movement data as the training data in Table IV.

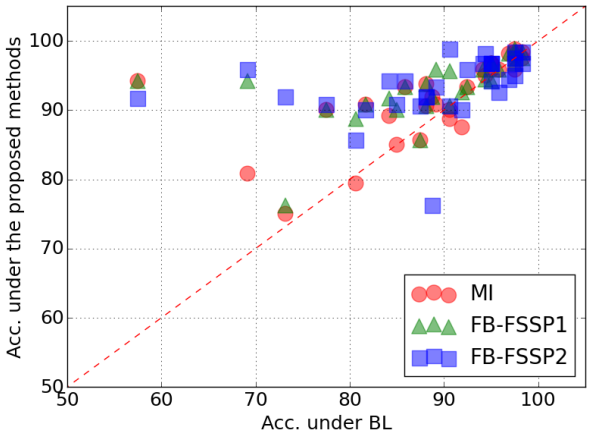

(a) Training data

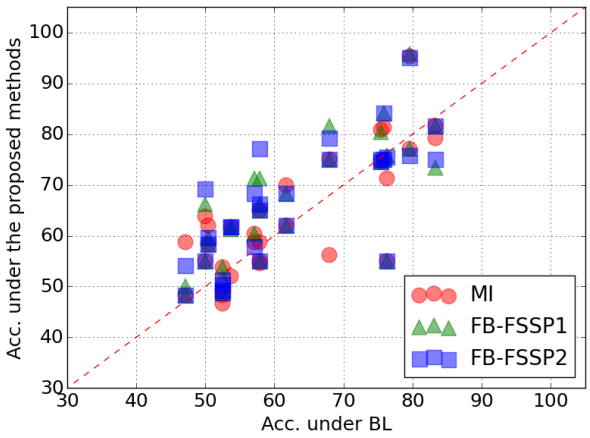

(b) Test data

Fig. 3. Classification results comparison.

As shown in Table IV, the spatial filter optimization methods based on Fisher's ratio outperform both the baseline and the mutual information spatial filter optimization with higher average and median values. Moreover, the significance of the improvements is validated by paired t-test with $\boldsymbol{p}$-values for both "FB-FSSP1" and "FB-FSSP2" below 0.05. For both settings, the training and test data were recorded on different days, resulting in the significant session-to-session transfer data variation. In particular, the proposed method could still capture the common sensorimotor patterns despite the data-type transfer. Hence it can found that the proposed method yields a better model generalization and is robust against both the and the data-type transfer.

The comparison results are illustrated more clearly in Figure 3, where the x-axis represents the results of FBCSP, the y-axis represents that of the other three methods in Table IV, and each dot marks one subject. Therefore, the more dots above the $x = y$ line, the more improvements achieved by the proposed method compared to FBCSP. It is found that both FB-FSSP1 and FB-FSSP2 achieve significant improvements for training data. For the test data, it still can be seen that FB-FSSP1 and FB-FSSP2 yield improvements although they are not as significant as that of the training data.

D. Discussion

1) Nonstationarity in Feature Space and Covariance Matrix Space: In this section, we investigate the objective functions in measuring the data non-stationarity. In the Fisher's ratio objective function, the within-class feature distances are calculated in a supervised manner as a measurement of data non-stationarity. Although mutual information is not explicitly used to address the non-stationarity issue when firstly adopted in FBCSP, feature distances are used to calculate the mutual information. For further analysis, we conduct a simulation study to investigate the relationship between feature distance and mutual information using the mutual information calculation in Appendix A.

Considering a set of 1-d feature f, let the mean features of class $+$ and $-$ be

$$\begin{aligned} \bar{f}^- &= 0.3 \\ \bar{f}^+ &= 0.7 \end{aligned} \tag{35}$$

which is a typical pair of averaged CSP features given the constraint $\bar{f}^- + \bar{f}^+ = 1$ in the optimization objective function Eq.(2). Assuming that $p(c) = 0.5$, we could calculate the mutual information between the class variable c and a 1-d feature f, $I(f, c)$, by using Eq.(36) to Eq.(41). The relationship between the feature f and mutual information $I(f, c)$ is illustrated in Figure 4, where the x-axis represents f, the y-axis represents $I(f, c)$, and the mean features of both classes are represented by two red dashed-dotted lines. $I(\mathbf{f}, c)$ calculated with the same h^c in Eq.(41) for both classes is shown in Figure 4 (a). It can be seen that symmetric about $f = 0.5$, $I(f, c)$ archives the minimal value when $f = 0.5$ and the larger the distance between f and 0.5, the higher the mutual information. In Figure 4 (b), we show examples of $I(f, c)$ when h^c are different for the two classes. It can be found that although the minimum is no longer $f = 0.5$, generally the mutual information is higher if the distance between f and 0.5 is larger. Different from the minimization of the within-class distances in the Fisher's ratio objective function, in the mutual information objective function, the distance between a feature and the feature boundary is maximized. With different h^c for different classes, it is likely that by maximizing mutual information, the feature is to be close to the center of one certain class. Moreover, as the calculation of mutual information is unsupervised, it cannot be guaranteed that the feature is closer to the center of the correct class. ~~This could be~~

TABLE IV
CLASSIFICATION RESULTS USING FILTER BANK (%)

	Training Acc.				Test Acc.			
Subject	FBCSP	$MI_s(MI_0)$	FB-FSSP1	FB-FSSP2	FBCSP	$MI_s(MI_0)$	FB-FSSP1	FB-FSSP2
M1	80.63	79.38	88.75	90.63	50.42	52.08	61.25	61.67
M2	89.17	90.83	95.83	94.17	60.42	58.75	50.00	54.17
M3	84.17	89.17	91.67	91.67	52.92	63.75	66.25	69.17
M4	94.17	95.83	95.83	96.67	71.25	54.58	71.25	77.08
M5	95.00	95.83	94.17	94.17	58.75	58.75	66.25	66.25
M6	97.50	95.83	96.67	96.67	83.33	81.25	84.17	84.17
M7	97.50	97.50	97.50	97.50	78.75	79.17	73.33	75.00
M8	98.33	98.33	98.33	98.33	96.25	95.42	95.83	95.00
M9	94.38	95.00	94.38	94.38	69.17	70.00	68.33	68.33
M10	85.00	85.00	90.00	90.00	65.00	62.08	59.58	59.58
M11	69.17	80.83	94.17	90.83	51.25	46.67	51.67	50.42
M12	92.50	93.33	93.33	92.50	79.58	80.83	80.42	75.00
M13	73.13	75.00	76.25	76.25	49.58	48.33	48.75	48.75
M14	90.63	88.75	95.63	95.00	75.00	71.25	75.83	75.42
M15	91.88	87.50	92.50	91.88	62.92	58.75	71.25	68.33
M16	90.63	90.00	90.63	91.88	71.67	56.25	81.66	79.17
P1	87.50	85.63	85.63	90.63	53.75	61.67	61.67	61.67
P2	85.83	93.33	93.33	94.17	47.08	48.33	48.33	54.17
P3	57.50	94.17	94.17	91.67	50.00	55.00	55.00	69.17
P4	95.00	96.67	96.67	96.67	57.92	65.00	65.00	77.08
P5	95.00	96.67	96.67	94.17	57.92	55.00	55.00	66.25
P6	95.00	96.67	96.67	96.67	75.83	75.00	75.00	84.17
P7	97.50	98.33	98.33	97.50	83.33	81.67	81.67	75.00
P8	98.33	97.50	97.50	98.33	79.58	77.08	77.08	95.00
P9	96.88	98.13	98.13	94.38	61.67	62.08	62.08	68.33
P10	81.67	90.83	90.83	90.00	50.42	58.33	58.33	59.58
P11	77.50	90.00	90.00	90.83	52.50	53.75	53.75	50.42
P12	95.83	95.83	95.83	92.50	75.42	74.58	74.58	75.00
P13	88.75	91.88	91.88	76.25	52.50	49.17	49.17	48.75
P14	97.50	98.75	98.75	95.00	76.25	55.00	55.00	75.42
P15	88.13	93.75	93.75	91.88	57.08	60.42	60.42	68.33
P16	88.13	90.63	90.63	91.88	67.92	75.00	75.00	79.17
mean	89.06	92.09	93.57	93.52	62.45	63.91	66.03	65.89
median	91.25	93.54	94.17	94.17	57.92	61.04	65.63	65.63
p-value	-	**0.02**	**0.003**	**0.008**	-	0.28	**0.01**	**0.02**

~~the reason why using mutual information to optimize spatial filters or select features are not as effective as Fisher's ratio.~~

While Fisher's ratio and mutual information are objective functions formulated in feature space, Rayleigh coefficient and KL-divergence can be regarded as that in covariance matrix space. When the non-stationarity is not considered in the objective function, maximizing Rayleigh coefficient or KL-divergence is equivalent to maximizing the mean inter-class distance due to the joint-diagonalization of the average covariance matrices from the two classes. When the non-stationarity is addressed by the regularization term in Eq.(8) based on Eq.(4), the solution can no longer jointly diagonalize the covariance matrices and the off-diagonal elements also contribute to the objective function in Eq.(7). However, only diagonal elements are used as features for classification, which means that there is a gap between the features optimized in the spatial filter design and that those used for classification.

To further investigate such inconsistency, the relationship between KL-divergence and feature distance is illustrated in Figure 5, where each dot marks one trial from the training data of the subject indicated in the figure. The x-axis represents $||\mathbf{d}||$ in Eq.(17) and y-axis represents the KL-divergence between a trial and the average EEG distribution from the same class after projection based on CSP, i.e., $D_{kl}(WR_jW^T||WR^cW^T)$ with $j \in \mathcal{Q}^c$. Moreover, linear regression between the KL-divergence and $||\mathbf{d}||$ is conducted, the result of which is also shown in Figure 5. It can be seen that the correlation between KL-divergence and feature distance is not very clear, and the resultant correlation coefficients are not significant in any of the three examples. Given that only diagonal elements are used as features, the KL-divergence objective function is less directly related to classification accuracy in feature space. This could explain why using KL-divergence to select features is not as effective as Fisher's ratio and mutual information. Yet, it is possible that addressing the non-stationarity in the covariance matrix space is less prone to over-fitting problem compared to the Fisher's ratio objective function, as the Fisher's ratio spatial filter optimization achieves more significant improvements in training accuracy than that in test accuracy.

2) Feature Distribution: In our previous work in [27], it is shown that the CSP features from two classes can be modeled as two Gamma distributions. It is proved that the Bayes error could be minimized by maximizing the Rayleigh quotient of the covariance matrices of the two classes under

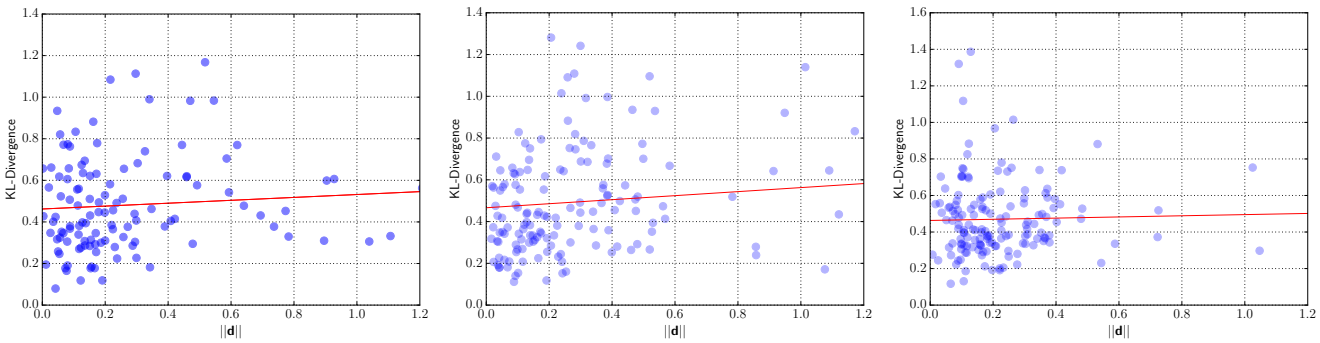

(a) Subject 7 (b) Subject 13 (c) Subject 14

Fig. 5. Relationship between KL-divergence and $||\mathbf{d}||$.

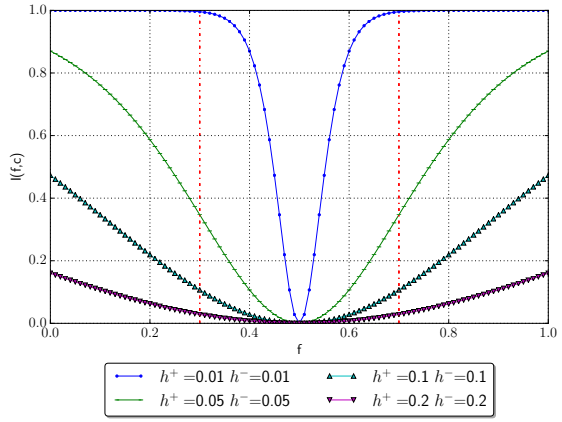

(a)

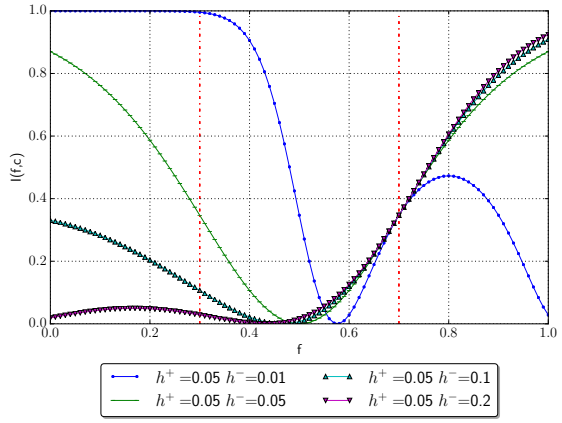

(b)

Fig. 4. Mutual information as a function of f.

the assumptions that 1) the two Gamma distributions have the same shape parameter, and 2) the shape parameter is a constant independent of the spatial filter. By simplifying the relationship between the shape parameter and the spatial filter, the within-class dissimilarity has not been addressed sufficiently. Thus, in this work, we approach to the problem with Fisher's ratio so that both inter-class and within-class dissimilarity could be taken into consideration. Yet, the assumption that the features follow normal distribution could be one limitation of the proposed method, and we expect that there would be a more comprehensive Bayes learning of the spatial filter.

3) Optimization: We investigate the subjects for whom the proposed method fails to achieve improvements. It is found that for some subjects, the subspace optimization converges at the very beginning of the searching, which yields results similar to FBCSP. Given that U_m is initialized as the discriminative subspace of the CSP solution, it is possible that the CSP solution is the optimized one, or there is a local minimum so that the searching cannot continue. In our future work, we would conduct more analysis to improve the subspace searching.

4) Relationship with Other Methods: In OSSFN proposed in [26], mutual information is used as the objective function of both temporal and spatial filters design by optimizing coefficient vectors of a group of subspace spatial filters, i.e., CSP or FBCSP spatial filters. In this work, we propose to search the subspace on manifold with Fisher's ratio or mutual information as objective function. Moreover, OSSFN adopts a "deflation" approach by optimizing the coefficient vectors one by one, which is proved to be less effective than the subspace gradient searching on manifolds [23].

The temporal filters are also optimized using SVM objective function and Rayleigh coefficient objective function in ISSPL and DFBCSP, respectively, while in FBCSP a soft-optimization approach is adopted by selecting the bands with higher mutual information [16], [15], [24], [25]. Compared to searching globally optimized temporal filters, the computational complexity of the soft-optimization approach is much lower with comparable results. Thus, in this work, we follow FBCSP by optimizing the temporal filters using the selection strategy. Moreover, in existing joint-temporal-spatial filter optimization methods, usually different objective functions are used for temporal and spatial filter optimization, feature selection, and classification. In the proposed method shown in Figure 1, Fisher's ratio is used for spatial filter optimization, feature selection and classification, which leads to a more unified model.

V. Conclusion

For practical BCI systems, how to optimize spatial filters to extract discriminative EEG features and be robust against EEG non-stationarity is one of the most challenging issues in spatial filter design. Given various objective functions and joint-temporal-spatial analysis methods, the relationship between different optimization methods and feature classification has not been sufficiently investigated.

In this work, we propose a novel spatial filter design method, which directly addresses both inter-class and within-class feature dissimilarity based on the Fisher's ratio as the objective function. The proposed method is a unified framework as the spatial filter optimization is directly formulated in the feature space, and the inconsistency between spatial filtering and feature extraction could be avoided. In addition, the proposed method does not require regularization parameter selection which needs to be conducted by cross-validation in regularization-based stationary spatial filter design. We implement the proposed method on both single broad band filter and filter bank with feature selection, and it is shown that Fisher's ratio objective function improves classification accuracy for both spatial filter design and feature selection. We also present a systematic attempt to compare it with different objective functions used for feature extraction and feature selection. With experimental and simulation studies, we discuss the advantages and disadvantages of different objective functions.

Appendix A
Mutual Information Objective Function

In [24], [25], mutual information objective function is used for soft-optimization by selecting the best spatial filters yielding the highest mutual information. In this work, we propose to optimize the subspace U_m to maximize the mutual information between class label variables c and feature variable $\mathbf{f}$ as shown in Eq.(36), i.e.,

$$I(\mathbf{f}, c) = H(c) - H(c|\mathbf{f}) \tag{36}$$

where

$$H(c) = \sum_{c\in\mathcal{C}} p(c)\log_2 p(c), \tag{37}$$

and

$$H(\mathcal{C}|\mathbf{f}) = -\frac{1}{m}\frac{1}{|\mathcal{Q}^c|}\sum_{i=1}^{m}\sum_{j\in\mathcal{Q}^c}\sum_{c\in\mathcal{C}} p(c|\mathbf{f}_{j,i})\log(p(c|\mathbf{f}_{j,i})) \tag{38}$$

$p(c|\mathbf{f}_{j,i})$, which is the conditional probability of class c given feature $\mathbf{f}_{j,i}$, can be computed as

$$p(c|\mathbf{f}_{j,i}) = \frac{p(\mathbf{f}_{j,i}|c)P(c)}{\sum_{c=+,-} p(\mathbf{f}_{j,i}|c)} \tag{39}$$

The conditional probability of $\mathbf{f}_{j,i}$ given class c, $p(\mathbf{f}_{j,i}|c)$, can be estimated using Gaussian function as

$$\begin{aligned} p(\mathbf{f}_{j,i}|c) &= \varphi(\mathbf{f}_{j,i} - \bar{\mathbf{f}}_i^c, h_i^c) \\ &= \varphi(\mathbf{d}_{j,i}^c, h_i^c) \end{aligned} \tag{40}$$

where

$$\varphi(\mathbf{d}, h) = \frac{1}{\sqrt{2\pi}} e^{-\frac{||\mathbf{d}||}{h^2}} \tag{41}$$

The smoothing parameter h_i^c can be calculated as

$$h_i^c = \left(\frac{4}{3|\mathcal{Q}^c|}\right)^{0.2}\sigma_i^c \tag{42}$$

where σ_i^c is the standard deviation of the i-th dimension of features belonging to class c.

Thus, with Eq.(36) to Eq.(42), the subspace U_m can be optimized using the following optimization objective function

$$\hat{U}_m = \arg\max_{U_m} J_{mi}(U_m) \text{ s.t. } U_m^T U_m = I \tag{43}$$

where

$$J_{mi}(U_m) = I(\mathbf{f}, c) \tag{44}$$

Remark 3: In [24], [25], $p(\mathbf{f}_{j,i}|c)$ is estimated using Parzen window. To reduce the computation complexity of calculating the gradient, we adopt a simplified way to estimate it as $p(\mathbf{f}_{j,i}|c)$ as shown in Eq.(40).

References

[1] H. Cecotti, M. P. Eckstein, and B. Giesbrecht, "Single-trial classification of event-related potentials in rapid serial visual presentation tasks using supervised spatial filtering," *IEEE Transactions on Neural Networks and Learning Systems*, vol. 25, no. 11, pp. 2030–2042, Nov 2014.

[2] F. Qi, Y. Li, and W. Wu, "Rstfc: A novel algorithm for spatio-temporal filtering and classification of single-trial EEG," *IEEE Transactions on Neural Networks and Learning Systems*, vol. 26, no. 12, pp. 3070–3082, Dec 2015.

[3] A. Y. Kaplan, A. A. Fingelkurts, S. V. Borisov, and B. S. Darkhovsky, "Nonstationary nature of the brain activity as revealed by EEG/MEG: methodological, practical and conceptual challenges," *Signal Process*, vol. 85, pp. 2109–2212, 2005.

[4] Dennis J. McFarland, Laurie A. Miner, Theresa M. Vaughan, and Jonathan R. Wolpaw, "Mu and beta rhythm topographies during motor imagery and actual movements," *Brain Topography*, vol. 12, pp. 177–186, 2000.

[5] J. R. Wolpaw, N. Birbaumer, W. J. Heetderks, D. J. McFarland, P. H. Peckham, G. Schalk, E. Donchin, L. A. Quatrano, C. J. Robinson, and T. M. Vaughanr, "Brain-computer interface technology: A review of the first international meeting," *IEEE Transactions on Rehabilitaion Engineering*, vol. 8, no. 2, pp. 164–173, 2000.

[6] "AR spectral analysis of EEG signals by using maximum likelihood estimation," *Computers in Biology and Medicine*, vol. 31, no. 6, pp. 441–450, 2001.

[7] V. Gandhi, G. Prasad, D. Coyle, L. Behera, and T. M. McGinnity, "Quantum neural network-based eeg filtering for a brain-computer interface," *IEEE Transactions on Neural Networks and Learning Systems*, vol. 25, no. 2, pp. 278–288, Feb 2014.

[8] J. Lu, K. Xie, and D.J. McFarland, "Adaptive spatio-temporal filtering for movement related potentials in EEG-based brain-computer interfaces," *IEEE Transactions on Neural Systems and Rehabilitation Engineering*, vol. 22, no. 4, pp. 847–857, July 2014.

[9] M. D. Fox, A. Z. Snyder, J. L. Vincent, and M. E. Raichle, "Intrinsic fluctuations within cortical systems account for intertrial variability in human behavior," *Neuron*, vol. 56, pp. 171–184, 2007.

[10] F. de Pasquale, S. D. Penna, A. Z. Snyder, C. Lewis, D. Mantini, L. Marzetti, P. Belardinelli, L. Ciancetta, V. Pizzella, G. L. Romani, and M. Corbetta, "Temporal dynamics of spontaneous MEG activity in brain networks," *Proceedings of the National Academy of Sciences*, vol. 107, pp. 6040–6045, 2010.

[11] Z. J. Koles, "The quantitative extraction and toporraphic mapping of the abnormal components in the clinical EEG," *Electroencephalography and Clinical Neurophysiology*, vol. 79, pp. 440–447, 1991.

[12] J. M. Gerkinga, G. Pfurtscheller, and H. Flyvbjergc, "Designing optimal spatial filters for single-trial EEG classiffication in a movement task," *Clinical Neurophysiology*, vol. 110, pp. 787–798, 1999.

[13] G. Pfurtscheller and A. Aranibar, "Evaluation of event-related desynchronization (ERD) preceding and following voluntary self-paced movements," *Electroencephalography and Clinical Neurophysiology*, vol. 46, no. 2, pp. 138–146, 1979.
[14] G. Pfurtscheller, C. Brunner, A. Schlol, and F.H. Lopes da Silva, "Mu rhythm (de)synchronization and EEG single-trial classification of different motor imagery tasks," *NeuroImage*, vol. 31, no. 1, pp. 153–159, 2006.
[15] H. Higashi and T. Tanaka, "Simultaneous design of fir filter banks and spatial patterns for EEG signal classification," *IEEE Transactions on Biomedical Engineering*, vol. 60, no. 4, pp. 1100–1110, April 2013.
[16] W. Wu, X. Gao, B. Hong, and S. Gao, "Classifying single-trial EEG during motor imagery by iterative spatio-spectral patterns learning (ISSPL)," *IEEE Transactions on Biomedical Engineering*, vol. 55, no. 6, pp. 1733–1743, June 2008.
[17] X. Li, H. Zhang, C. Guan, S. H. Ong, K. K. Ang, and Y. Pan, "Discriminative learning of propagation and spatial pattern for motor imagery EEG analysis," *Neural Computation*, vol. 25, no. 10, pp. 2709–2733, 2013.
[18] X. Li, C. Guan, H. Zhang, K. K. Ang, and S. H. Ong, "Adaptation of motor imagery EEG classification model based on tensor decomposition," *Journal of Neural Engineering*, vol. 11, pp. 056020, 2014.
[19] F. Lotte and C. Guan, "Regularizing common spatial patterns to improve BCI designs: Unified theory and new algorithms," *IEEE Transactions on Biomedical Engineering*, vol. 58, no. 2, pp. 355–362, 2011.
[20] W. Samek, C. Vidaurre, K.-R. Müller, and M. Kawanabe, "Stationary common spatial patterns for brain-omputer interfacing," *Journal of Neural Engineering*, vol. 9, no. 2, pp. 026013, March 2012.
[21] W. Samek, F.C. Meinecke, and K.-R. Müller, "Transferring subspaces between subjects in brain-computer interfacing," *IEEE Transactions on Biomedical Engineering*, vol. 55, no. 3, pp. 902–913, March 2008.
[22] M. Arvaneh, C. Guan, K. K. Ang, and C. Quek, "Optimizing spatial filters by minimizing within-class dissimilarities in electroencephalogram-based brain computer interface," *IEEE Transactions on Neural Networks and Learning Systems*, vol. 24, no. 4, pp. 610–619, June 2013.
[23] W. Samek, M. Kawanabe, and K.-R. Müller, "Divergence-based framework for common spatial patterns algorithms," *IEEE Reviews in Biomedical Engineering*, vol. 7, pp. 50–72, 2013.
[24] K. K. Ang, Z. Y. Chin, C. Wang, C. Guan, and H. Zhang, "Filter bank common spatial pattern algorithm on BCI competition IV datasets 2a and 2b," *Frontiers in Neuroscience*, vol. 6, no. 39, 2012.
[25] K. K. Ang, Z. Y. Chin, H. Zhang, and C. Guan, "Mutual information-based selection of optimal spatial-temporal patterns for single-trial EEG-based BCIs," *Pattern Recognition*, vol. 45, no. 6, pp. 2137–2144, 2012.
[26] H. Zhang, Z. Y. Chin, K. K. Ang, C. Guan, and C. Wang, "Optimum spatio-spectral filtering network for brain-computer interface," *IEEE Transactions on Neural Networks*, vol. 22, no. 1, pp. 52–63, Jan 2011.
[27] H. Zhang, H. Yang, and C. Guan, "Bayesian learning for spatial filtering in an EEG-based brain-computer interface," *IEEE Transactions on Neural Networks and Learning Systems*, vol. 24, no. 7, pp. 1049–1060, 2013.
[28] M. D. Plumbley, "Geometrical methods for non-negative ica: Manifolds, lie groups and toral subalgebras," *Neurocomputing*, vol. 67, pp. 161 – 197, 2005.
[29] K. K. Ang, C. Guan, C. Wang, K. S. Phua, A. H. G. Tan, and Z. Y. Chin, "Calibrating EEG-based motor imagery brain-computer interface from passive movement," *2011 Annual International Conference of the IEEE on Engineering in Medicine and Biology Society, EMBC*, pp. 4199–4202, 2011.